Nonlinear Dynamics of Multibody Systems Using an Augmented Lagrangian Formulation

Nikolaos Potosakis, Elias Paraskevopoulos, and Sotirios Natsiavas

Abstract A class of multibody systems subject to bilateral scleronomic motion constraints is investigated. The formulation is based on a new set of equations of motion, expressed as a coupled system of strongly nonlinear second-order ordinary differential equations. After putting these equations in a weak form, the position, velocity, and momentum type quantities are assumed to be independent, leading to a three-field set of equations of motion. Next, an equivalent augmented Lagrangian formulation is set up by introducing a set of penalty terms. This final set of equations is then used as a basis for developing a new time integration scheme, which is applied to several example systems. In those examples, special emphasis is put on illustrating the advantages of the new method when applied to mechanical systems, involving redundant constraints or singular configurations.

Keywords Analytical mechanics · Multibody dynamics · Bilateral motion constraints · Weak form of equations of motion · Augmented Lagrangian

1 Introduction

Research on multibody dynamics helps in developing more efficient and robust numerical techniques for solving challenging engineering problems. This in turn yields useful design gains in many areas, including mechanisms, robotics, biomechanics, automotive, railway, and aerospace structures [1–4]. Typically, the equations of motion for this class of systems are derived and cast in the form of a set of differential-algebraic equations (DAEs) of high index. Earlier attempts to solve these equations are based on index reduction or coordinate partitioning techniques [3, 4]. In contrast, the main objective of this chapter is to first create and employ

N. Potosakis · E. Paraskevopoulos · S. Natsiavas (✉)
Department of Mechanical Engineering, Aristotle University, Thessaloniki, Greece
e-mail: natsiava@auth.gr

W. Lacarbonara et al. (eds.), *Nonlinear Dynamics of Structures, Systems and Devices*, https://doi.org/10.1007/978-3-030-34713-0_1

a better theoretical foundation and then proceed to development of more advanced numerical schemes.

In the new approach, the equations of motion employed are second-order ordinary differential equations (ODEs). This is achieved by combining concepts of Analytical Dynamics and differential geometry and leads to a natural elimination of singularities associated with DAE formulations from the onset [5]. Since the ulterior motive is the development of an efficient numerical integration scheme, these equations are first put in a convenient weak form. Moreover, the position, velocity, and momentum type quantities are assumed to be independent, forming a three-field set of equations [6]. Finally, the set of equations obtained is solved by application of an augmented Lagrangian formulation, which is set up after introducing appropriate penalty terms [7]. Next, the validity and efficiency of this scheme is tested and illustrated by applying it to a number of characteristic example mechanical systems.

The set of equations of motion employed is included in Sect. 2. Originally, they appear in a strong form and are subsequently put in a three-field weak form. After introducing penalty terms, they are cast eventually in an augmented Lagrangian form. Then, a temporal discretization scheme is developed and numerical results are presented for two mechanical examples in Sect. 3.

2 Equations of Motion: Augmented Lagrangian Formulation

This chapter employs a new set of equations of motion, obtained for a class of multibody mechanical systems subject to equality constraints. The motion is described by a finite number of generalized coordinates $q = (q^1 \dots q^n)$, at any time t [1, 2]. In this way, it can be represented by the motion of a fictitious point, say p, along a curve on the n-dimensional configuration manifold M of the system. Moreover, the tangent vector $\underset{\sim}{v}$ to this curve belongs to an n-dimensional vector space T_pM, the tangent space of manifold M at p [2]. The systems examined are subject to a set of k motion constraints. For simplicity, these constraints are assumed to be scleronomic, with form

$$\dot{\psi}^R \equiv a_i^R(q)\dot{q}^i = 0. \tag{1}$$

When a constraint is holonomic, its equation can be integrated in the algebraic form

$$\phi^R(q) = 0. \tag{2}$$

The equations of motion of the class of systems examined can be cast in the form

$$\underset{\sim}{h}^* \equiv \underset{\sim}{h}_M^* - \underset{\sim}{h}_C^* = \underset{\sim}{0} \tag{3}$$

on manifold M, where

$$\underset{\sim}{h}^*_M = h_i \, \underset{\sim}{e}^i \quad \text{with} \quad h_i = \left(g_{ij} v^j\right)^{\cdot} - \Lambda^m_{\ell i} g_{mj} v^j v^\ell - f_i \tag{4}$$

and

$$\underset{\sim}{h}^*_C = \sum\nolimits_{R=1}^{k} h_R a_i^R \, \underset{\sim}{e}^i \quad \text{with} \quad h_R = \left(\overline{m}_{\mathrm{RR}} \dot{\lambda}^R\right)^{\cdot} + \overline{c}_{\mathrm{RR}} \dot{\lambda}^R + \overline{k}_{\mathrm{RR}} \lambda^R - \overline{f}_R. \tag{5}$$

In Eq. (5), the summation convention on repeated indices does not apply to index R. Moreover, the coefficients $\overline{m}_{\mathrm{RR}}$, $\overline{c}_{\mathrm{RR}}$, $\overline{k}_{\mathrm{RR}}$, and $\overline{f}_R$ are determined by the constraints [5]. Equation (3) represents a set of n second-order coupled strongly nonlinear ODEs in the $n + k$ unknowns q^i and λ^R. A complete mathematical formulation is obtained by incorporating the k equations of the constraints, which are expressed originally by Eqs. (1) and (2). In particular, these equations are replaced eventually by

$$g_R = \left(\overline{m}_{\mathrm{RR}} \dot{\phi}^R\right)^{\cdot} + \overline{c}_{\mathrm{RR}} \dot{\phi}^R + \overline{k}_{\mathrm{RR}} \phi^R = 0 \quad \text{and} \quad g_R = \left(\overline{m}_{\mathrm{RR}} \dot{\psi}^R\right)^{\cdot} + \overline{c}_{\mathrm{RR}} \dot{\psi}^R = 0, \tag{6}$$

respectively, for $R = 1, \ldots, k$ [5].

Taking into account Eq. (3) leads first to

$$\int_{t_1}^{t_2} \left(\underset{\sim}{h}^*_M - \underset{\sim}{h}^*_C\right)\left(\underline{w}\right) \mathrm{d}t = 0, \quad \forall \underline{w} \in T_p M, \tag{7}$$

along a natural trajectory on the manifold and within any time interval $[t_1, t_2]$. Moreover, as variation of a function f is defined the derivative of f along vector $\underline{w}$, by

$$\delta f \equiv \underline{w}(f) = f_i w^i. \tag{8}$$

Then, $w^i = \delta q^i$ for each holonomic coordinate, while a little more involved relation is obtained in case of nonholonomic coordinates [6]. In addition, the position, velocity, and momentum variables are considered as independent quantities in the sequel. For this, a new velocity field $\underline{\upsilon}$ is introduced on manifold M, which should eventually be forced to become identical to the true velocity field $\underline{v}$. This means that

$$\upsilon^i = v^i \Rightarrow \delta \upsilon^i = \delta v^i, \tag{9}$$

with variations defined through Eq. (8) by $\delta \upsilon^i = \underline{w}\left(\upsilon^i\right)$ and $\delta v^i = \underline{w}\left(v^i\right)$. In analogy to the action leading to Eq. (7), conditions (9) are imposed by

$$\int_{t_1}^{t_2} \left[\delta\pi_i \left(\upsilon^i - v^i \right) + \pi_i \left(\delta\upsilon^i - \delta v^i \right) \right] \mathrm{d}t = 0, \tag{10}$$

where the quantities $\delta\pi_i$ and π_i are components of co-vectors belonging to the cotangent space $T_p^* M$. In the same spirit, by considering the motion constraints expressed by Eq. (6), the following relation must also be satisfied

$$\int_{t_1}^{t_2} g_R \, \delta\lambda^R \mathrm{d}t = 0, \tag{11}$$

for an arbitrary multiplier $\delta\lambda^R$ and each $R = 1, \ldots, k$. Then, integrating by parts the first term in the integrand for a holonomic constraint yields

$$\left(\overline{m}_{\mathrm{RR}} \dot{\phi}^R \delta\lambda^R \right) \Big|_{t_1}^{t_2} - \int_{t_1}^{t_2} \left[\overline{m}_{\mathrm{RR}} \dot{\phi}^R \left(\delta\lambda^R \right)^{\cdot} - \left(\overline{c}_{\mathrm{RR}} \dot{\phi}^R + \overline{k}_{\mathrm{RR}} \phi^R \right) \delta\lambda^R \right] \mathrm{d}t = 0, \tag{12}$$

while a similar result is also obtained for a nonholonomic constraint.

Next, a similar action is also taken for the velocity components $\dot{\lambda}^R$, by introducing a new vector field on $T_{p_R} M_R$ for each constraint manifold M_R, with components μ^R, together with a new set of Lagrange multipliers σ_R, belonging to the cotangent space $T_{p_R}^* M_R$. As a consequence, the weak formulation is augmented by the terms

$$\int_{t_1}^{t_2} \left[\delta\sigma_R \left(\mu^R - \dot{\lambda}^R \right) + \sigma_R \left(\delta\mu^R - \delta\dot{\lambda}^R \right) \right] \mathrm{d}t = 0, \quad (R = 1, \ldots, k), \tag{13}$$

where $\delta\sigma_R$ represents the component of a co-vector on $T_{p_R}^* M_R$. Then, one can relate the strong time derivatives v^i (of q^i or ϑ^i, for a true or a pseudo-coordinate, respectively) and $\dot{\lambda}^R$ of the position type variables to weak velocities, denoted by υ^i and μ^R, through two new sets of Lagrange multipliers, denoted by $\delta\pi_i$ and $\delta\sigma_R$, respectively.

Finally, appending the terms in Eqs. (10)–(13) to Eq. (7) and performing lengthy manipulations leads eventually to an involved three-field set of equations [6]. Then, since the variations w^i, $\delta\lambda^R$, $\delta\upsilon^i$, $\delta\mu^R$, $\delta\pi_i$, and $\delta\sigma_R$ are independent, collecting the terms in these equations multiplied by these quantities leads to a coupled set of nonlinear algebraic equations. In fact, by adding suitable penalty terms due to the constraints, it is found that the form of these equations remains unaffected, making the substitution

$$\overline{\mu}^R = \mu^R - \xi_R \dot{\phi}^R \quad \text{and} \quad \overline{\lambda}^R = \lambda^R - \xi_R \phi^R, \tag{14}$$

when μ^R and λ^R is multiplied by $\overline{m}_{\mathrm{RR}}$ or $\overline{c}_{\mathrm{RR}}$ and $\overline{k}_{\mathrm{RR}}$, respectively. This provides a convenient and strong basis for developing an appropriate temporal discretization of the equations of motion. For the purposes of the present chapter, this task was

performed within the framework of the augmented Lagrangian formulation, leading to a convenient block-type iterative technique within each time step.

3 Numerical Results

Some characteristic results are presented next for two selected examples. The first example is of academic interest, while the second corresponds to an industrial application.

3.1 Planar Slider-Crank Mechanism

First, in Fig. 1 are compared results obtained by applying the new method with similar results reported for a typical benchmark problem [8]. The planar slider-crank mechanism shown in the inset of Fig. 1b is examined. This represents multibody systems passing through a singular configuration. The two rods have an equal length of 1 m and a uniformly distributed mass of 1 kg, while the slider has a negligible mass and is constrained to move along the ground axis Ox. Consequently, the number of degrees of freedom increases instantaneously from one to two when

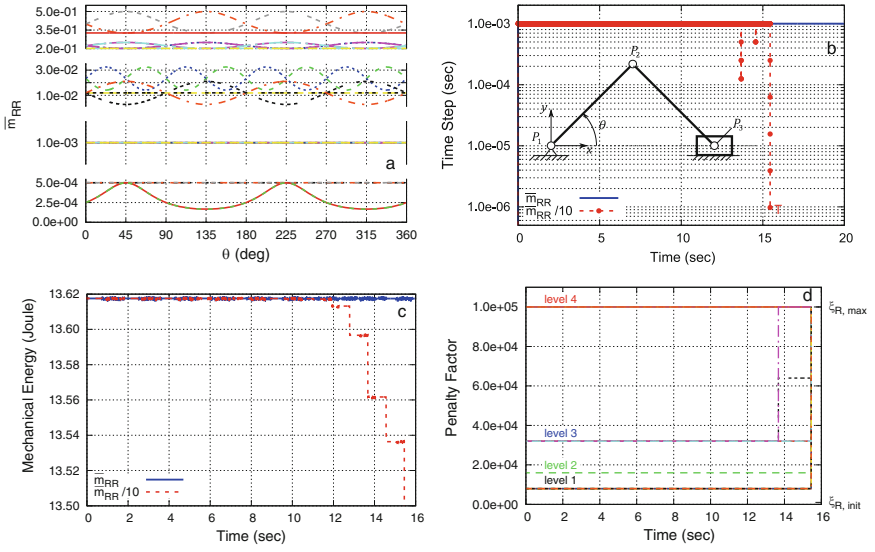

Fig. 1 Results for a slider-crank mechanism: (**a**) values of $\overline{m}_{\mathrm{RR}}$ as a function of θ, (**b**) time step variation for $\overline{m}_{\mathrm{RR}}$ and $\overline{m}_{\mathrm{RR}}/10$, (**c**) mechanical energy for $\overline{m}_{\mathrm{RR}}$ and $\overline{m}_{\mathrm{RR}}/10$, and (**d**) changes in the values of the penalty factors leading to convergence up to about 16 s for $\overline{m}_{\mathrm{RR}}/10$

$\theta = n\pi/2$, with $n = 0, 1, \ldots$. The mechanism starts from the position with $\theta = \pi/4$, so that the initial velocity of point P_3 is 4 m/s along the $-x$ direction and executes oscillations due to the action of gravity, acting along the $-y$ direction, with gravity acceleration equal to 9.81 m/s^2.

Based on standard modeling requirements, the model employed consists of four rigid bodies, corresponding to 24 dof. In addition, it is subject to a total of $k = 26$ bilateral constraints. This means that three of these constraints are redundant. First, in Fig. 1a are presented the values of all the $\overline{m}_{\mathrm{RR}}$ parameters, obtained over a full rotation of the two members. A significant variation is observed to occur in the value of $\overline{m}_{\mathrm{RR}}$ for some of the constraints over the complete rotation. In addition, a much bigger difference is observed in the values from one constraint to another. Next, in Fig. 1b is shown the time step history. When the correct values were selected for $\overline{m}_{\mathrm{RR}}$ the step was found to remain constant and equal to the initial selection. Also, some of the penalty factors kept their initial value ($\xi_R = 1000$), while some other were increased up to 2000. However, when a wrong value of $\overline{m}_{\mathrm{RR}}/10$ was selected, instead, the time step decreased occasionally and eventually fell below the minimum allowable value. In Fig. 1c is shown the corresponding mechanical energy of the system, showing an observable drop in its value at times where a decrease in the time step is performed. Also, the penalty values had to be increased by two orders of magnitude when $\overline{m}_{\mathrm{RR}}/10$ was selected, as depicted in Fig. 3d. Moreover, even that increase was not sufficient to guarantee continuation of the simulation beyond the first 16 s of the motion.

Next, in Fig. 2a, b are shown the time step and the mechanical energy of the mechanism, by using the correct values of $\overline{m}_{\mathrm{RR}}$ but keeping the same constant penalty values for all the constraints. The results indicate that a convergence is possible to occur in the numerical solution, within the time interval examined, provided that the penalty values lie within a specific interval (here 10^3–10^4). The explanation for this behavior is that for an excessive value of the penalty value, the part associated with the corresponding constraint term dominates the Jacobian matrix of the resulting set of linear algebraic equations at each iteration step, leading to ill-conditioning. On the other hand, relatively small values of the penalty factors make a small contribution to the Jacobian matrix and this implies that a larger number of iteration is required for convergence at each step.

Likewise, in Fig. 2c, d are shown the same quantities, obtained as a function of time for the correct values of $\overline{m}_{\mathrm{RR}}$, by keeping constant all the penalty factors to their initial values, again. Moreover, the results of the new method, represented by the dashed line, are compared to those obtained by applying the same method after setting $\overline{m}_{\mathrm{RR}} = 0$, $\overline{c}_{\mathrm{RR}} = 0$, $\overline{k}_{\mathrm{RR}} = 1$ and $\overline{f}_R = 0$ in Eq. (5), so that $h_R = \lambda^R$. In addition, it was also set $\overline{m}_{\mathrm{RR}} = 1$ in Eq. (6). In this way, the set of equations employed is reduced to the set of equations of motion employed by current multibody dynamics formulations [9, 10]. This case is referred to as a modified augmented Lagrangian formulation (M-ALF). Comparison of the results shows that the numerical performance gets worse, demonstrating the advantages associated with the new set of equations of motion.

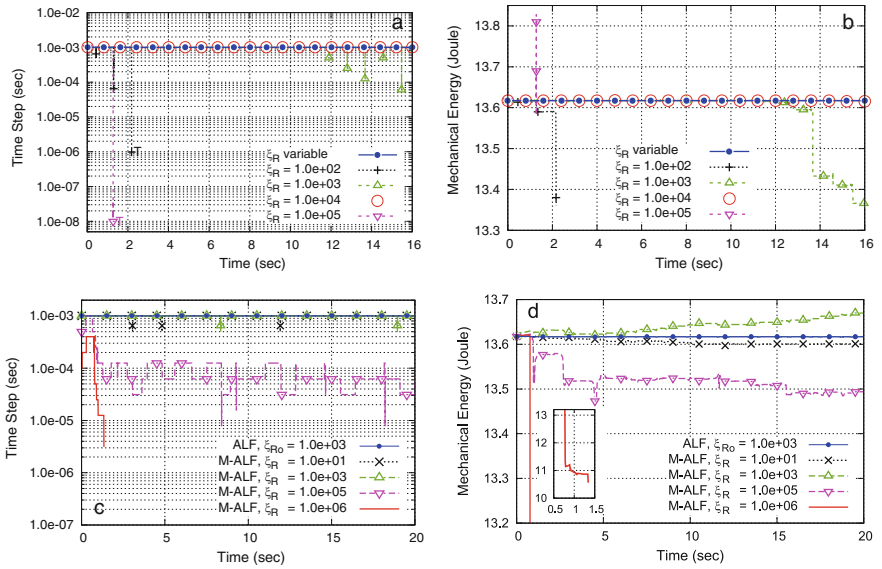

Fig. 2 Numerical results for a slider-crank mechanism: (**a**) time step variation, (**b**) mechanical energy for different constant values of the penalty factors, (**c**) time step variation, and (**d**) mechanical energy obtained by the modified augmented Lagrangian formulation (M-ALF)

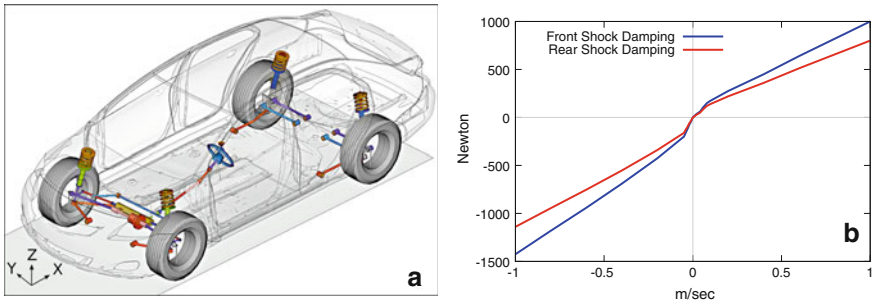

Fig. 3 (**a**) Complete vehicle model and (**b**) forces in the front and rear shock dampers as a function of relative velocity

3.2 Complex Model of a Ground Vehicle

In the second example, a model of a real ground vehicle was examined, shown in Fig. 3a. Many of its components exhibit strongly nonlinear behavior. For instance, in Fig. 3b are shown the forces developed in the front and rear shock dampers as a function of the relative velocity. Finally, the tires were modeled using the Pacejka tire model. In total, the model consists of 53 rigid bodies, interconnected with 49 kinematical constraints, 29 bushings, 9 spring-damper systems, and 9 action-reaction force elements. As a consequence, the total number of degrees of freedom of the final model is 134.

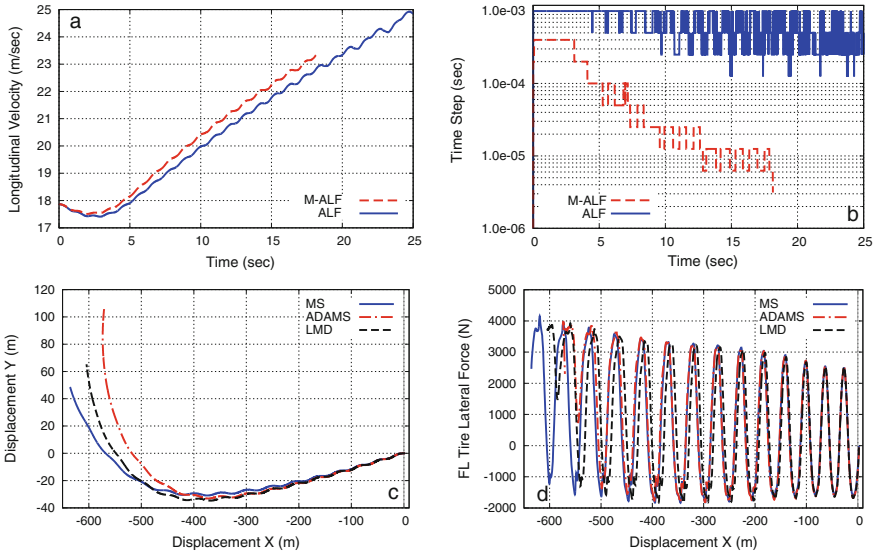

Fig. 4 Results for a repeated swept steering maneuver: (**a**) history of the longitudinal velocity of the car, (**b**) size of the time step, (**c**) comparison of trajectories, and (**d**) comparison of tire lateral forces obtained with two BDF solvers

The vehicle was subjected to a repeated swept steering maneuver, by applying a torque at the car's differential and imposing the steering angle imposed on the steering wheel during the motion. First, in Fig. 4a is shown the history of the longitudinal velocity of the car. The results of the new method are represented by the continuous curve. These results are first compared with those obtained by applying the modified augmented Lagrangian formulation (M-ALF), as was defined in Sect. 3.1. In the latter case, a sudden interruption of the time integration occurred after about 17 s of motion, as indicated by the broken curve. The reason for this interruption is explained by the results of Fig. 4b, where the size of the time step employed by the two methods is shown. Besides this, the results illustrate that the new method, using variable penalty factors and correct values for the parameters $\overline{m}_{\mathrm{RR}}$, $\overline{c}_{\mathrm{RR}}$, $\overline{k}_{\mathrm{RR}}$, and $\overline{f}_R$, leads to substantially smaller time steps, especially as the duration of the event increases. Next, in Fig. 4c is shown a comparison of the resulting car trajectories on the horizontal plane, obtained by two state of the art commercial codes [11, 12]. These codes set up the equations of motion and solves them numerically as a system of index-3 DAEs by employing a classical integration scheme, based on backward differentiation formulas (BDF). Likewise, Fig. 4d presents a comparison of the corresponding lateral force developed in the front left tire. Here, the deviations observed between the results of the new method and the codes grow gradually and become large at the final stages of the maneuver.

References

1. Greenwood, D.T.: Principles of Dynamics. Prentice-Hall Inc., Englewood Cliffs (1988)
2. Bloch, A.M.: Nonholonomic Mechanics and Control. Springer, New York (2003)
3. Geradin, M., Cardona, A.: Flexible Multibody Dynamics. Wiley, New York (2001)
4. Bauchau, O.A.: Flexible Multibody Dynamics. Springer, London (2011)
5. Natsiavas, S., Paraskevopoulos, E.: A set of ordinary differential equations of motion for constrained mechanical systems. Nonlinear Dyn. **79**, 1911–1938 (2015)
6. Paraskevopoulos, E., Natsiavas, S.: Weak formulation and first order form of the equations of motion for a class of constrained mechanical systems. Int. J. Non linear Mech. **77**, 208–222 (2015)
7. Bertsekas, D.P.: Constraint Optimization and Lagrange Multiplier Methods. Academic Press, New York (1982)
8. IFToMM TC for Multibody Dynamics, Library of Computational Benchmark Problems. http://www.iftomm-multibody.org/benchmark
9. Bayo, E., Ledesma, R.: Augmented Lagrangian and mass-orthogonal projection methods for constrained multibody dynamics. Nonlinear Dyn. **9**, 113–130 (1996)
10. Dopico, D., Gonzalez, F., Cuadrado, J., Kovecses, J.: Determination of holonomic and nonholonomic constraint reactions in an index-3 augmented Lagrangian formulation with velocity and acceleration projections. ASME J. Comput. Nonlinear Dyn. **9**, 041006 (2014)
11. MSC Adams, User Guide. MSC Software Corporation, Newport Beach (2016)
12. MotionSolve v14.0, User Guide. Altair Engineering Inc., Irvine